IEEE Access
Multidisciplinary ⋮ Rapid Review ⋮ Open Access Journal

Received July 25, 2020, accepted August 8, 2020, date of publication August 19, 2020, date of current version August 31, 2020.

*Digital Object Identifier 10.1109/ACCESS.2020.3017759*

# Four-Wheel Differential Steering Control of IWM Driven EVs

**JIE TIAN[1], JIE DING[1], CHUNTAO ZHANG[1], AND SHI LUO[2]**
[1]College of Automobile and Traffic Engineering, Nanjing Forestry University, Nanjing 210037, China
[2]College of Automobile and Traffic Engineering, Jiangsu University, Zhengjiang 212013, China

Corresponding author: Jie Tian (njtianjie@163.com)

This work was supported in part by the National Natural Science Foundation of China under Grant 51975299 and Grant 11272159, in part by the National Youth Foundation of China under Grant 51305207, and in part by the High Level Talent Fund of Nanjing Forestry University under Grant GXL2018004.

**ABSTRACT** This paper aims to realize the four-wheel differential steering function of an in-wheel motor (IWM) driven electric vehicle (EV) with a steer-by-wire (SBW) system. The dynamic models of four-wheel differential steering vehicle (4WDSV) and four-wheel steering vehicle (4WSV) are established, and a front-wheel steering vehicle (2WSV) with the neutral steering characteristics and a drop filter of the sideslip angle is employed as the reference model to provide the ideal yaw rate and sideslip angle. According to the reference model, the decoupling and fractional $PI^{\lambda}D^{\mu}$ controllers are designed for the 4WSV to obtain the standard inputs, i.e., the front and rear wheel steering angles, which is finally drawn as the MAP. Furthermore, the sliding mode controller (SMC) and torque distributor are designed to control the 4WDSV to have the same yaw rate as the 4WSV, whose inputs are consulted from the MAP drawn in advance according to the vehicle speed. The simulation results of several vehicle models with/without the controller of two working conditions (reverse and in phase steering) are presented, which indicates that the proposed decoupling and fractional $PI^{\lambda}D^{\mu}$ controller for the 4WSV is effective to obtain its standard inputs, and the proposed SMC and torque distributor for the 4WDSV ensure that it has the same yaw rate as the 4WSV, as well as the good robustness.

**INDEX TERMS** Four-wheel differential steering, in-wheel motor driven, decoupling, fractional $PI^{\lambda}D^{\mu}$ control, sliding model control.

## I. INTRODUCTION

In recent decades, the in-wheel motor (IWM) driven technology of electric vehicles (EV) becomes one of the significant breakthrough in today's automobile industry [1]. Each IWMs can be controlled independently and their drive information can be obtained quickly and accurately, which makes the design of dynamic control system more convenient and flexible, and the driving force of each wheel more rational [1], [2]. Therefore, the appearance of the four-wheel IWM driven EV opens up the possibility of the differential steering system (DSS), which can be easily achieved by controlling of the left and right wheel driving torques.

Up to now, there are three functions of the DSS: (1) Steering the vehicle without the lateral turning of the wheel, that is, the skid steering [3], [4]; (2) Assisting the driver to steer the vehicle and reducing the driver's load, i.e., the differential drive assisted steering (DDAS) [5]–[8]; (3) Steering the vehicle in case of the failure [9]–[15] or instead of the regular steering system [16]–[18]. Among them, the literatures [9]–[18] are most related to this study.

The differential steering was used as an emerging steering mechanism when the regular steering system was defective. Considering the desired front-wheel steering angle was uncertain and hard to obtain, a robust $H_{\infty}$ output-feedback controller based on the front-wheel DSS was designed to achieve the yaw stabilization and parametric uncertainties for the cornering stiffness and the external disturbances were considered to guarantee the vehicle robustness. The effectiveness of the proposed controller to guarantee the equal handling and stability was verified by the simulation results [9]. A front-wheel DSS was utilized to actuate the front wheels to achieve the path following control when the regular steering system failed. And a multiple-disturbances observer-based composite nonlinear feedback (CNF) approach was proposed to improve the transient performance of the fault-tolerant control with the DSS, and the disturbance observer was

The associate editor coordinating the review of this manuscript and approving it for publication was Chao Yang.

designed to estimate the external disturbances with unknown bounds. The effectiveness of the proposed controller was evaluated by the simulation results [10].

To realize the yaw control when the active front steering entirely breaks down, an integral sliding mode control (ISMC) was proposed for the IWM EV steered by the DSS. A disturbance observer based ISMC strategy was designed to deal with the unknown mismatched disturbances and the composite nonlinear feedback technique was applied to design the controller's nominal part. The simulation results evaluated the effectiveness of the proposed control approach in the case of the steering failure [11]. A sliding mode controller (SMC) based on the reference model for the front-wheel differential steering vehicle (DSV) was presented when the regular steering system failed. Simulation results showed that the designed controller can not only control the yaw rate and sideslip angle of vehicle to track those of the reference model exactly, but also ensure the robustness of the controlled system compared with the designed controller for the skid steering vehicle (SSV) [12].

Considering a stuck fault in the active front-wheel steering, the front-wheel DSS was used to achieve the normal steering and the path-following task. An adaptive triple-step control approach with the consideration of parameter uncertainties for the cornering stiffness and external disturbances was proposed to realize the lateral and longitudinal path following of IWM driven autonomous ground vehicles (AGVs). And the effectiveness of the proposed scheme was evaluated [13]. With the front-wheel DSS, the stability problem for IWM EVs was handled to avoid dangerous consequences for vehicles when the regular steering system was in failure. To ensure the efficiency of the DSS, vehicle rollover prevention was considered to balance the vertical load of the two-side wheels. And the $H_\infty$observer-based feedback control strategy was employed to handle the measurement problem of the reference front wheel steering angle and lateral velocity [14]. When the active-steering motor completely failed, the DSS generated by the differential moment between the front wheels was used to steer the vehicle. An adaptive multivariable super-twisting control algorithm was proposed to achieve the lane keeping control. And the effectiveness and robustness of the proposed approach were verified by the simulation results [15].

A new steer-by-wire concept only using the DSS was presented. A planar vehicle model with the DSS was derived. At high speed, a full state feedback linear control system based on linear quadratic regulator (LQR) principle was proposed to achieve the four-wheel DSS. While at low speed, a simple PI angle controller was developed to realize the front-wheel DSS. Various simulation experiments demonstrated that the steering performance of the DSS was comparable to that of conventional passenger cars [16]. As the sole steering system, a DSS was investigated to generate the effect of the conventional steering mechanism (CSM) via the input torque of the four wheels. Based on the linear vehicle model, the DSS which combines the forward speed and yaw rate controllers was designed using the $H_\infty$ control method. Simulation results showed that the DSS can realize the vehicle maneuvering under different working conditions by tracking the expected parameters without using any CSM [17]. A self-steering four-wheel independent EV was designed, which can turn around only keeping the different speed of the left and right wheels. Its control model was obtained from the kinematic model and dynamic model deducted by force analysis, which had been compared with Ackermann-Jeantand steering model. Traditional proportion-integration-differentiation (PID) feedback control loop was employed to track the reference torque of four independent wheels. The steering system was tested in the actual muddy agriculture field and the results were verified using a prototype and real vehicle [18].

In summary, literatures [9]–[15] only used the DSS as the emergency or spare steering system once the regular steering systems failed, furthermore they utilized only front wheel as the sole steering input. In fact, the DSS can also be served as a unique steering system and can even be extended to the four-wheel steering. Because the DSS is achieved by the differential driving torque between the left and right wheels, it is no necessary to add any dedicated steering device. However, in literatures [16]–[18], the four-wheel DSS as the unique steering system was realized by controlling the speed of each wheel, and then the required driving torque of each wheel can be obtained.

In order to make the driver have the same feeling as driving the traditional front wheel steering vehicle when the vehicle adopts the four-wheel DSS, in this paper the traditional front-wheel steering vehicle with the neutral steering characteristics and a drop filter of the sideslip angle is used as the reference model to provide the required steering wheel angle. Then a four-wheel steering vehicle (4WSV) model is introduced. By the decoupling and fractional $PI^\lambda D^\mu$ control, the 4WSV can have the same response as the reference model and provide the ideal front and rear wheel steering angles for the distribution of the front and rear differential driving torque of the four-wheel differential steering vehicle (4WDSV). Finally, through the SMC, the 4WDSV can have the same yaw rate as the reference model. This method to achieve the four-wheel DSS is very different from the normal tracking control of the speed of each wheel.

Therefore, the main contributions of this paper are: 1) Replacing the normal 4WSV with a more flexible four-wheel DSS, which uses the differential driving torques of the front and rear wheels as the control inputs. 2) For the 4WDSV, a new control method is provided, instead of tracking the speed of each wheel. 3) According to the reference model, the decoupling and fractional $PI^\lambda D^\mu$ controllers of the 4WSV are designed to obtain the MAP of the standard inputs of the 4WSV. 4) The SMC and torque distributor are designed to control the 4WDSV to have the same yaw rate as the 4WSV, whose inputs can be consulted from the MAP drawn in advance according to the vehicle speed and the steering angle of the steering wheel.

The article structure is as follows: The 4WDSV, 4WSV and reference models are presented in Section II. Section III describes the control strategy of the 4WDSV. Section IV is the method to acquire the MAP of the front and rear wheel steering angles for the 4WSV, including the designs of the decoupling and fractional $PI^{\lambda}D^{\mu}$ controller. The SMC and torque distributor for the 4WDSV are designed in Section V. Simulation results are reported in Section VI. Finally, the conclusion is summarized in Section V.

## II. VEHICLE MODELS

In this section, we will first present three models, the 4WDSV model whose inputs are the front and rear wheel differential driving torques, 4WSV model and reference model.

### A. MODEL OF 4WDSV

For the 4WDSV studied in this paper, there is no mechanical connection between the steering wheel and four wheels of the vehicle, in which four hub motors are installed. The driver's intention is provided to the electronic control unit (ECU) through the steering wheel, which gives instructions to the left and right hub motors of the front and rear axles and achieves the corresponding differential steering according to the collected signals and internal control procedures.

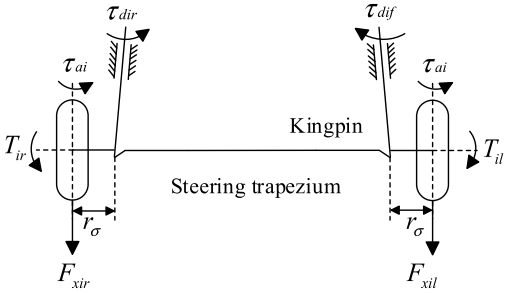


**FIGURE 1.** Steering mechanism of 4WDSV.

The two sets of the front and rear steering mechanisms are identical and Fig. 1 shows one of the steering mechanisms, where $T_{ij}$ $(i = f, r, j = l, r)$ is the driving torque of the front/rear left/right wheel, $F_{xij}$ $(i = f, r, j = l, r)$ is the driving force of the front/rear left/right wheel, $\tau_{dij}$ $(i = f, r, j = l, r)$ is the torque of the front/rear left/right wheel around the kingpin generated by $F_{xij}$, $\tau_{ai}$ $(i = f, r)$ is the aligning torque of the front/rear wheel, $r_\sigma$ is the scrub radius.

For either of the steering mechanisms, $\tau_{dij}$ will force the wheel to rotate towards the longitudinal centerline of the vehicle because of the scrub radius $r_\sigma$, therefore $\tau_{dil}$ and $\tau_{dir}$ are in the opposite directions. Due to the steering trapezium between the left and right wheels, when the driving torque of the left and right wheels is equal, the wheels will not produce the steering angle; when the driving torque of the two wheels is not equal, the steering mechanism will drive the wheels to turn to the side with the smaller driving torque.

The forces acting on the vehicle body are shown in Fig. 2, where $\delta_i$ $(i = f, r)$ is the front/rear wheel steering angle;

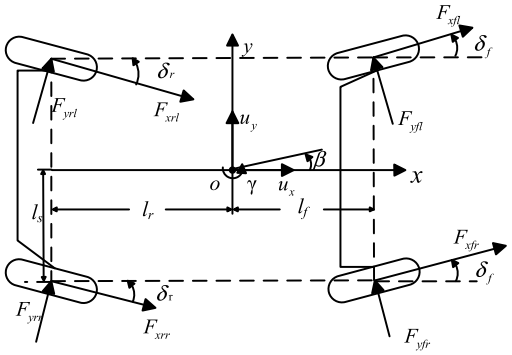


**FIGURE 2.** Dynamic model of 4WDSV.

$F_{yij}$ $(i = f, r, j = l, r)$ is the tire lateral force of the front/rear left/right wheel; $l_s$ is the half of the front/rear tire contact length; $\beta$ is the sideslip angle; $\gamma$ is the yaw rate; $u_x$ and $u_y$ are the longitudinal and lateral velocities at the center of gravity (CG), respectively; $l_f$ and $l_r$ are the distances from the center of mass to the front and rear axle, respectively. For the 4WSVs, the front and rear wheels can rotate in the same or opposite direction. In Fig. 2, the front wheel steering angle is positive, and the rear wheel steering angle is negative, the lateral and yaw motion of the 4WDSV can be expressed as:

$$\begin{cases} mu_x(\dot{\beta}+\gamma) = (F_{yfl}+F_{yfr})\cos\delta_f + (F_{xfl}+F_{xfr})\sin\delta_f \\ \qquad + (F_{yrl}+F_{yrr})\cos\delta_r + (F_{xrl}+F_{xrr})\sin\delta_r \\ I_Z\dot{\gamma} = (l_f\sin\delta_f + l_s\cos\delta_f)\frac{\Delta M_f}{R} \\ \qquad + (l_f\cos\delta_f - l_s\sin\delta_f)(F_{yfl}+F_{yfr}) \\ \qquad + (l_r\sin\delta_r + l_s\cos\delta_r)\frac{\Delta M_r}{R} \\ \qquad - (l_r\cos\delta_r - l_s\sin\delta_r)(F_{yrl}+F_{yrr}) \end{cases} \tag{1}$$

where $R$ is the wheel radius, $k_i$ $(i = f, r)$ is the front/rear tire cornering stiffness, $\Delta M_i$ $(i = f, r)$ is the differential driving torque of the front/rear axle and

$$\Delta M_i = (F_{xir} - F_{xil})R, \quad F_{yfj} = k_f\alpha_f, \quad F_{yrj} = k_r\alpha_r,$$
$$\alpha_f = \beta + l_f\gamma/u_x - \delta_f, \quad \alpha_r = \beta - l_r\gamma/u_x - \delta_r.$$

Considering that the tire cornering stiffness always fluctuates due to the change of loads and road conditions, they can be expressed as

$$k_f = k_{f0} + \Delta k_f, \quad k_r = k_{r0} + \Delta k_r \tag{2}$$

where $k_{f0}$ and $k_{r0}$ are the nominal values of the front and rear tire cornering stiffness, $\Delta k_f$ and $\Delta k_r$ are the corresponding perturbation values.

Define $x(t) = \begin{bmatrix}\beta & \gamma\end{bmatrix}^T$, $u(t) = \Delta M = \Delta M_f + \Delta M_r$, $f_1(t) = \delta_f, f_2(t) = \delta_r$, (1) can be written as

$$\dot{x} = (A + \Delta A)x + Bu + D_1f_1 + D_2f_2 \tag{3}$$

where $\Delta A$ is the perturbation matrix of $A$, and

$$A = \begin{bmatrix} \frac{2\left(k_{f0}+k_{r0}\right)}{mu_x} & \frac{2\left(l_f k_{f0}-l_r k_{r0}\right)}{mu_x^2}-1 \\ \frac{2\left(l_f k_{f0}-l_r k_{r0}\right)}{I_z} & \frac{2\left(l_f^2 k_{f0}+l_r^2 k_{r0}\right)}{I_z u_x} \end{bmatrix},$$

$$\Delta A = \begin{bmatrix} \frac{2(\Delta k_f+\Delta k_r)}{mu_x} & \frac{2\left(l_f \Delta k_f-l_r \Delta k_r\right)}{mu_x^2} \\ \frac{2\left(l_f \Delta k_f-l_r \Delta k_r\right)}{I_z} & \frac{2\left(l_f^2 \Delta k_f+l_r^2 \Delta k_r\right)}{I_z u_x} \end{bmatrix},$$

$$B = \begin{bmatrix} 0 \\ \frac{l_s}{RI_z} \end{bmatrix},\ D_1 = \begin{bmatrix} -\frac{2k_{f0}}{mu_x} \\ -\frac{2k_{f0}l_f}{I_z} \end{bmatrix},\ D_2 = \begin{bmatrix} -\frac{2k_{r0}}{mu_x} \\ -\frac{2k_{r0}l_r}{I_z} \end{bmatrix}.$$

### B. MODEL OF 4WSV

In order to obtain $\Delta M$ of the 4WDSV, the 4WSV model is introduced. To simplify the dynamic model of the 4WSV for the controller design, only the planar motion is taken into account without considering the pitch and roll motions. The 4WSV is simplified as a single track model, as shown in Fig. 3.

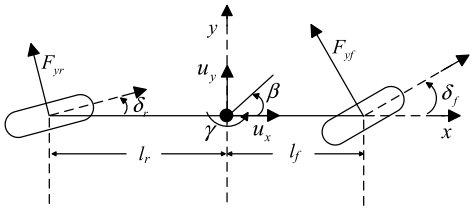


**FIGURE 3.** Dynamic model of 4WSV.

The lateral and yaw motion of the 4WSV can be expressed as:

$$\begin{cases} mu_x(\dot{\beta}+\gamma) = F_{yf}\cos\delta_f + F_{yr}\cos\delta_r \\ I_Z\dot{\gamma} = l_f F_{yf}\cos\delta_f - l_r F_{yr}\cos\delta_r \end{cases} \tag{4}$$

where $F_{yi}(i=f,r)$ is the tire lateral force of the front/rear wheel and $F_{yi} = k_{i0}\alpha_i$.

When the front and rear steering angles are small, the linear equations of (4) can be written as:

$$\begin{cases} mu_x(\dot{\beta}+\gamma) = 2(k_{f0}+k_{r0})\beta + \frac{2(l_f k_{f0}-l_r k_{r0})}{u_x}\gamma \\ \quad -2k_{f0}\delta_f - 2k_{r0}\delta_r \\ I_Z\dot{\gamma} = 2\left(l_f k_{f0}-l_r k_{r0}\right)\beta + \frac{2\left(l_f^2 k_{f0}+2l_r^2 k_{r0}\right)}{u_x}\gamma \\ \quad -2l_f k_{f0}\delta_f + 2l_r k_{r0}\delta_r \end{cases} \tag{5}$$

Define $x_d(t) = \left[\beta_d\ \gamma_d\right]^T$, $u_{d1}(t) = \delta_f$, $u_{d2}(t) = \delta_r$, the state equation is expressed as:

$$\dot{x}_d = A_d x_d + B_{d1}u_{d1} + B_{d2}u_{d2} \tag{6}$$

where

$$A_d = \begin{bmatrix} \frac{2(k_{f0}+k_{r0})}{mu_x} & \frac{2\left(l_f k_{f0}-l_r k_{r0}\right)}{mu_x^2}-1 \\ \frac{2\left(l_f k_{f0}-l_r k_{r0}\right)}{I_z} & \frac{2\left(l_f^2 k_{f0}+l_r^2 k_{r0}\right)}{I_z u_x} \end{bmatrix} = \begin{bmatrix} a_{11} & a_{12} \\ a_{21} & a_{22} \end{bmatrix},$$

$$B_{d1} = \begin{bmatrix} -\frac{2k_{f0}}{mu_x} \\ -\frac{2l_f k_{f0}}{I_z} \end{bmatrix} = \begin{bmatrix} b_{11} \\ b_{21} \end{bmatrix},\ B_{d2} = \begin{bmatrix} -\frac{2k_{r0}}{mu_x} \\ \frac{2l_r k_{r0}}{I_z} \end{bmatrix} = \begin{bmatrix} b_{12} \\ b_{22} \end{bmatrix}.$$

The matrix transfer function of the system with the state-representation (6) is given by

$$\begin{bmatrix} \beta_d(s) \\ \gamma_d(s) \end{bmatrix} = \begin{bmatrix} G_{11}(s) & G_{12}(s) \\ G_{21}(s) & G_{22}(s) \end{bmatrix}\begin{bmatrix} \delta_f(s) \\ \delta_r(s) \end{bmatrix} \tag{7}$$

where

$$G_{11}(s) = \frac{sb_{11}-a_{22}b_{11}+a_{12}b_{21}}{s^2-(a_{11}+a_{22})s+a_{11}a_{22}-a_{21}a_{12}},$$
$$G_{12}(s) = \frac{sb_{12}-a_{22}b_{12}+a_{12}b_{22}}{s^2-(a_{11}+a_{22})s+a_{11}a_{22}-a_{21}a_{12}},$$
$$G_{21}(s) = \frac{sb_{21}-a_{11}b_{21}+a_{21}b_{11}}{s^2-(a_{11}+a_{22})s+a_{11}a_{22}-a_{21}a_{12}},$$
$$G_{22}(s) = \frac{sb_{22}-a_{11}b_{22}+a_{21}b_{12}}{s^2-(a_{11}+a_{22})s+a_{11}a_{22}-a_{21}a_{12}}.$$

### C. REFERENCE MODEL

Up to now, there is no conclusion about the reference model. There are usually two kinds of the reference model, one is the first-order system with zero sideslip angles, and the other is the front wheel steering (FWS) vehicle with neutral steering. And it is also believed that the driver will not adapt to zero sideslip angle. In this paper, the 2DOF FWS vehicle with a neutral steering characteristics and a sideslip angle filter is used as the reference model to provide the reference sideslip angle and yaw rate.

For the reference model, it differs from the 4WSV in that it has the neutral steering characteristics, and the rear wheels cannot be steered. When the tire stiffness of the reference model and 4WSV are the same, the steering characteristics of the reference model can be easily adjusted to the neutral by adjusting the distances from the center of mass to the front and rear axles. Assuming that $\delta$ is the front wheel steering angle of the reference model, $l_{fm}$ and $l_{rm}$ are the distances of the reference model from the center of mass to the front and rear axle, respectively, the lateral and yaw motions can be expressed from (5) as follows when $\delta_r$ is set to be zero.

$$\begin{cases} mu_x(\dot{\beta}+\gamma) = 2(k_{f0}+k_{r0})\beta + \frac{2(l_{fm}k_{f0}-l_{rm}k_{r0})}{u_x}\gamma - 2k_{f0}\delta \\ I_Z\dot{\gamma} = 2\left(l_{fm}k_{f0}-l_{rm}k_{r0}\right)\beta + \frac{2\left(l_{fm}^2 k_{f0}+2l_{rm}^2 k_{r0}\right)}{u_x}\gamma - 2l_{fm}k_{f0}\delta \end{cases} \tag{8}$$

Define $x_m(t) = \left[\beta_m\ \gamma_m\right]^T$, $u_{m1}(t) = \delta$, the 2DOF 2WS vehicle with the neutral steering characteristics can be

described as,

$$\dot{x}_m = A_m x_m + B_m u_{m1} \tag{9}$$

where

$$A_m = \begin{bmatrix} \dfrac{2(k_{f0}+k_{r0})}{mu_x} & \dfrac{2\left(l_{fm}k_{f0}-l_{rm}k_{r0}\right)}{mu_x^2}-1 \\ \dfrac{2\left(l_{fm}k_{f0}-l_{rm}k_{r0}\right)}{I_z} & \dfrac{2\left(l_{fm}^2k_{f0}+l_{rm}^2k_{r0}\right)}{I_z u_x} \end{bmatrix},$$

$$B_m = \begin{bmatrix} -\dfrac{2k_{f0}}{mu_x} \\ -\dfrac{2l_{fm}k_{f0}}{I_z} \end{bmatrix}.$$

And the drop filter of the sideslip angle is as follows,

$$G_d(s) = \frac{\eta\omega_n^2}{s^2+\sqrt{2}\omega_n+\omega_n^2} \tag{10}$$

where $\eta$ is the gain coefficient that can be used to adjust the amplitude of the sideslip angle, $\omega_n$ is the cutoff frequency, and $s$ is the complex variable.

## III. PROBLEM FORMULATION

For the 4WDSV, its steering is achieved by the differential driving torque between the left and right wheels of the front and rear axles, which is very different from the normal 4WSV. And we hope it has the same yaw rate as the reference model. Therefore, we propose the control block diagram as shown in Fig. 4.

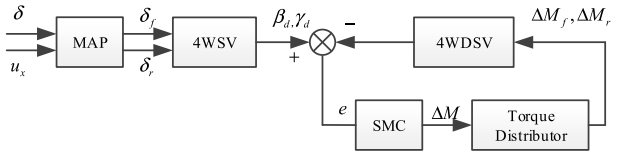


**FIGURE 4.** Control block diagram of 4WDSV.

According to the front wheel steering angle and vehicle speed of the reference model, the standard front and rear wheel steering angles of the 4WSV can be consulted in the MAP by the interpolation method firstly. Then the total differential driving torque, $\Delta M$, can be obtained by the SMC to ensure that the 4WDSV can track the yaw rate of the 4WSV, and the differential driving torque of the front and rear axles, $\Delta M_f$ and $\Delta M_r$, can be acquired by the torque distributor.

In addition, the MAP of the front and rear wheel steering angles is obtained in advance by the decoupling control block diagram as shown in Fig. 5. Specifically, we decouple the sideslip angle and yaw rate of the 4WSV by introducing two independent input variables, $u_1$ and $u_2$, and get the transfer functions of sideslip angle to $u_1$, and yaw rate to $u_2$. Then the fractional $PI^{\lambda}D^{\mu}$ controller is adopted to make the sideslip angle and yaw rate track those of the reference model, and the standard front and rear wheel angle of the 4WSV, $\delta_f$ and $\delta_r$, are obtained. When the vehicle speed is fixed and the front wheel steering angle of the reference model is changed,

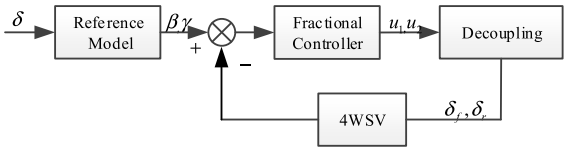


**FIGURE 5.** Method of getting MAP.

a series of front and rear wheel angles of 4WSV, i.e., MAP, can be obtained.

That is to say, in order to make the 4WDSV have the same yaw rate as the reference model, a series of controllers are needed. Firstly, the decoupling and fractional $PI^{\lambda}D^{\mu}$ controllers are required for the 4WSV to get the MAP of its front and rear wheel steering angles. Then the sliding mode controller and torque distributor for the 4WDSV are needed.

## IV. ACQUISITION OF MAP

The MAP in this paper refers to the curve of the standard front and rear wheel steering angles, which the 4WSV should have to obtain the same steering characteristics as the reference model at a specific speed. Here the decoupling and fractional $PI^{\lambda}D^{\mu}$ control is used to acquire the front and rear wheel steering angles. Then they are plotted into the MAP, and the corresponding front and rear wheel angles of the 4WSV can be obtained by the interpolation method.

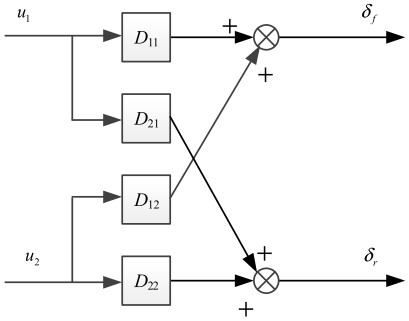


**FIGURE 6.** Decoupling of 4WSV.

### A. DECOUPLING OF 4WSV

From (7), we can see that the sideslip angle and yaw rate are controlled by both of the steering angles of the front and rear wheels. Therefore, two intermediate variables, $u_1$ and $u_2$ (shown in Fig. 6), are introduced to make the following equation hold.

$$\begin{pmatrix} \delta_f(s) \\ \delta_r(s) \end{pmatrix} = \begin{pmatrix} \mathrm{D}_{11}(s) & D_{12}(s) \\ D_{21}(s) & D_{22}(s) \end{pmatrix} \begin{pmatrix} u_1(s) \\ u_2(s) \end{pmatrix} \tag{11}$$

Only when

$$\begin{pmatrix} G_{11}(s) & G_{12}(s) \\ G_{21}(s) & G_{22}(s) \end{pmatrix} \begin{pmatrix} D_{11}(s) & D_{12}(s) \\ D_{21}(s) & D_{22}(s) \end{pmatrix} = \begin{pmatrix} G_{11}(s) & 0 \\ 0 & G_{22}(s) \end{pmatrix} \tag{12}$$

$\beta$ and $\gamma$ can be controlled by $u_1$ and $u_2$ respectively, and $D_{ij}$ can be obtained as follows by solving (12).

$$D_{11}(s)=\frac{b_2s^2+b_1s+b_0}{a_2s^2+a_1s+a_0},\quad D_{12}(s)=\frac{b_5s^2+b_4s+b_3}{a_2s^2+a_1s+a_0},$$
$$D_{21}(s)=\frac{b_8s^2+b_7s+b_6}{a_2s^2+a_1s+a_0},\quad D_{22}(s)=\frac{b_{11}s^2+b_{10}s+b_9}{a_2s^2+a_1s+a_0}.$$

where

$$\begin{aligned}
a_0 &= (a_{12}b_{21}-a_{22}b_{11})\,(a_{21}b_{12}-a_{11}b_{22}+a_{11}b_{12}-a_{12}b_{22}),\\
a_1 &= a_{21}b_{12}b_{11}-a_{11}b_{22}b_{11}+a_{11}b_{12}b_{21}-a_{12}b_{21}b_{12},\\
a_2 &= b_{11}b_{22}-b_{21}b_{12},\\
b_0 &= (a_{21}b_{12}-a_{11}b_{22})\,(a_{12}b_{21}-a_{22}b_{11}),\\
b_1 &= a_{21}b_{12}b_{11}-a_{11}b_{22}b_{11}+a_{12}b_{21}b_{22}-a_{22}b_{11}b_{22},\\
b_2 &= b_{22}b_{11},\\
b_3 &= (a_{11}b_{12}-a_{12}b_{22})\,(a_{21}b_{12}-a_{11}b_{22}),\\
b_4 &= -a_{21}b_{12}^2+a_{11}b_{22}b_{12}+a_{11}b_{12}b_{22}-a_{12}b_{22}^2,\\
b_5 &= -b_{12}b_{22},\\
b_6 &= (-a_{12}b_{21}+a_{22}b_{11})\,(a_{21}b_{11}-a_{11}b_{21}),\\
b_7 &= -a_{12}b_{21}^2+a_{22}b_{11}b_{21}-a_{21}b_{11}^2+a_{11}b_{11}b_{21},\\
b_8 &= -b_{11}b_{21},\\
b_9 &= (a_{21}b_{12}-a_{11}b_{22})\,(a_{12}b_{21}-a_{22}b_{11}),\\
b_{10} &= a_{21}b_{12}b_{11}-a_{11}b_{22}b_{11}+a_{12}b_{21}b_{22}-a_{22}b_{11}b_{22},\\
b_{11} &= b_{22}b_{11}.
\end{aligned}$$

### B. DESIGN OF FRACTIONAL $PI^{\lambda}D^{\mu}$ CONTROLLER

The fractional $PI^{\lambda}D^{\mu}$ controller, which is not sensitive to the system parameter uncertainty, is robust and can be designed flexibly. Its transfer function can be expressed as [19]

$$G_{cf}(s)=\frac{U(s)}{E(s)}=K_P+\frac{K_I}{s^{\lambda}}+K_Ds^{\mu} \tag{13}$$

where $K_P$, $K_I$ and $K_D$ are the proportional, integral and differential coefficients, respectively; $\lambda$ and $\mu$ are the integral and differential orders, respectively.

Fractional $PI^{\lambda}D^{\mu}$ may be tuned by finding parameters that satisfy the following conditions [20], where $G(s)$ represents $G_{11}(s)$ or $G_{22}(s)$.

$$\left|G_{cf}\left(\omega_{cg}\right)G\left(\omega_{cg}\right)\right|=0dB \tag{14}$$
$$-\pi+\phi_m=\arg\left[G_{cf}\left(\omega_{cg}\right)G\left(\omega_{cg}\right)\right] \tag{15}$$
$$\left|\frac{G_{cf}\left(\omega_h\right)G\left(\omega_h\right)}{1+G_{cf}\left(\omega_h\right)G\left(\omega_h\right)}\right|<H \tag{16}$$
$$\left|\frac{1}{1+G_{cf}\left(\omega_l\right)G\left(\omega_l\right)}\right|<N \tag{17}$$
$$\frac{d}{d\omega}\arg\left[G_{cf}\left(\omega_{cg}\right)G\left(\omega_{cg}\right)\right]\Big|_{\omega=\omega_{cg}}=0 \tag{18}$$

where $\omega_{cg}$ and $\phi_m$ are the gain-crossover frequency and phase margin, respectively; $\omega_h$ and $\omega_l$ are the specified frequencies, respectively; $H$ and $N$ are the specified gains, respectively.

When using the minimum of $\left|G_{cf}\left(\omega_{cg}\right)G\left(\omega_{cg}\right)\right|$ as the objective function and meeting the other four constraints, the particle swarm optimization algorithm can be used to get these five parameters $K_P$, $K_I$, $K_D$, $\lambda$and $\mu$.

In addition, the transfer function such as (13) are not easy to implement for computational purpose because simulations are usually carried out with the software only prepared to deal with integer transfer functions. Therefore, it is necessary to find the integer order approximations of the fractional transfer function, $s^{v}$. One of the best-known approximations is due to Oustaloup and is given by [21]

$$s^{v}_{[\omega_a\ \omega_b]}\cong K\prod_{i=-N}^{N}\frac{1+s/\omega_i}{1+s/\omega_i'} \tag{19}$$

where

$$K=\left(\frac{\omega_b}{\omega_a}\right)^{-\frac{v}{2}}\prod_{i=-N}^{N}\frac{\omega_i}{\omega_i'},\quad \omega_i'=\omega_a\left(\frac{\omega_b}{\omega_a}\right)^{\frac{i+N+0.5(1+v)}{2N+1}},$$
$$\omega_i=\omega_a\left(\frac{\omega_b}{\omega_a}\right)^{\frac{i+N+0.5(1-v)}{2N+1}}.$$

To use this approximation, the frequency range of $[\omega_a, \omega_b]$ and the number of zeros and poles $N$ should be fixed in advance. When the integer order approximation of fractional transfer functions was achieved, the simulation model can be easily built by MATLAB.

## V. CONTROL OF 4WDSV

For the 4WDSV, the SMC and torque distributor are needed to guarantee that it can have the same yaw rate of the 4WSV. Here the 4WSV is used as the reference model of the 4WDSV.

### A. DESIGN OF SMC

The purpose of the model reference control system is to require the state variables of the controlled object to track those of the reference model. The state variables of the error system can be defined as

$$e=x_d-x \tag{20}$$

From the controlled object (3) and the 4WSV model (6), the error model of the model reference control system can be obtained as follows

$$\begin{aligned}\dot{e}=A_de+(A_d-A)\,x+B_{d1}u_{d1}+B_{d2}u_{d2}\\ -Bu-(\Delta Ax+D_1f_1+D_2f_2)\end{aligned} \tag{21}$$

If regard (21) as the control object of the variable structure control system, and (22) as the external disturbance respectively,

$$\begin{aligned}\Delta=(A_d-A)\,x+B_{d1}u_{d1}+B_{d2}u_{d2}\\ -Bu-(\Delta Ax+D_1f_1+D_2f_2)\end{aligned} \tag{22}$$

the complete model tracking condition of model reference control system is equivalent to the invariant condition of variable structure control system.

For (21), select the whole sliding mode switching hyperplane

$$s(e,t)=Ce(t) \tag{23}$$

where $C$ is the sliding mode parameter matrix to be designed, and $C = \left[ C_1 \ C_2 \right], C_2 \in R^{m\times m}$ is nonsingular.

If the complete model tracking condition is satisfied, the equivalent system of sliding mode motion of the model reference variable structure adaptive control system is:

$$\dot{e} = \left\{ I - B\left[CB\right]^{-1} C \right\} A_d e \tag{24}$$

It can be seen that the closed-loop control system can achieve the complete model tracking. The structure of the model reference variable structure control law can be taken as

$$u = u_m + u_v = u_m + u_L + u_N \tag{25}$$

where $u_m$ is the matching control law of the model reference closed-loop control system, $u_v$ is the variable structure control law, $u_L$ is the variable structure linear control term, $u_N$ is the variable structure nonlinear control term.

According to the model matching conditions for complete tracking, there is a matching control law

$$u_m = K_d x + K_{d1} u_{d1} + K_{d2} u_{d2} \tag{26}$$

where $K_d \in R^{m\times n}, K_{d1} \in R^{m\times l}, K_{d2} \in R^{m\times l}$, and they satisfy $A_d - A = BK_d, B_{d1} = BK_{d1}$ and $B_{d2} = BK_{d2}$.

Therefore, after introducing the matching control law, (21) becomes,

$$\dot{e} = A_d e - Bu_v - \left(\Delta A x + D_1 f_1 + D_2 f_2\right) \tag{27}$$

Because $(A_d, -B)$ is a controllable matrix pair, there must be a nonsingular linear transformation to transform (27) into a controllable regular type according to the knowledge of matrix theory. And the nonsingular linear transformation is introduced,

$$z = Te = \begin{bmatrix} I_{n-m} & -B_1 B_2^{-1} \\ 0 & I_m \end{bmatrix} e \tag{28}$$

then

$$z = \begin{bmatrix} z_1 \\ z_2 \end{bmatrix}, \quad \tilde{A}_d = \begin{bmatrix} \tilde{A}_{d11} & \tilde{A}_{d12} \\ \tilde{A}_{d21} & \tilde{A}_{d22} \end{bmatrix}, \quad \tilde{B} = \begin{bmatrix} 0 \\ \tilde{B}_2 \end{bmatrix},$$
$$\Delta\tilde{A} = \begin{bmatrix} 0 & 0 \\ \Delta A_{21} & \Delta A_{22} \end{bmatrix}, \quad \tilde{D}_1 = \begin{bmatrix} 0 \\ D_1 \end{bmatrix}, \quad \tilde{D}_2 = \begin{bmatrix} 0 \\ D_2 \end{bmatrix},$$

where $z_1 \in R^{n-m}, z_2 \in R^m, \tilde{A}_{d11} \in R^{(n-m)\times(n-m)}, \tilde{A}_{d22} \in R^{m\times m}$ and $\tilde{B}_2 \in R^{m\times m}$.

The matching control law can be rewritten as

$$u_m = \tilde{B}_2^{-1} \left[ 0 \quad I_m \right] T \left(A_d - A\right) x + \tilde{B}_2^{-1} \left[ 0 \quad I_m \right] \times \left(B_{d1} u_{d1} + B_{d2} u_{d2}\right) \tag{29}$$

Assuming $\left\| \Delta A_{21} \ \Delta A_{22} \right\| \le \psi_\sigma, \left\| B_2^{-1} \right\| = \varphi \le 1$, the final sliding mode control law of the variable structure can be obtained as follows,

$$u_L = B_2^{-1} \left[ \tilde{A}_{d21} \quad \tilde{A}_{d22} - \tilde{A}^*_{d22} \right] Te \tag{30}$$

$$u_N = \rho\left(t\right) \frac{B_2^{-1} P \left[ 0 \quad I_m \right] T}{\left\| P \left[ 0 \quad I_m \right] T \right\|} \tag{31}$$

where $\tilde{A}^*_{d22}$ is Hurwitz matrix, symmetric positive definite matrixes, $\rho\left(t\right) = \left(1-\varphi\right)^{-1} \left[ \left(\psi_\sigma + \psi\right) \|x\| + \psi_{r1} \|u_{d1}\| + \psi_{r2} \|u_{d2}\| + \psi_e \|e\| + \psi_{d1}\psi_{f1} + \psi_{d2}\psi_{f2} \right] + \varepsilon, \psi_{r1} = \|K_{d1}\|, \psi_{r2} = \|K_{d2}\|, \psi = \|K\|, \psi_e = \left\| B_2^{-1} \left[ \tilde{A}_{d21} \ \tilde{A}_{d22} - \tilde{A}^*_{d22} \right] T \right\|, \psi_{d1} = \|D_1\|, \psi_{d2} = \|D_2\|, \psi_{f1} = \|f_1\|, \psi_{f2} = \|f_2\|, \varepsilon > 0$, $P$ and $Q$ are the symmetric positive definite matrixes, respectively, and satisfy Lyapunov Equation

$$P\tilde{A}^*_{d22} + \left(\tilde{A}^*_{d22}\right)^T P = -Q \tag{32}$$

### B. DESIGN OF TORQUE DISTRIBUTOR

Because the MAP diagram is drawn in advance, it is not difficult for us to get the ratio $k$ of the front and rear wheel angles of the 4WSV by consulting the MAP. And $k$ is positive when the front and rear wheel turn in the same direction, otherwise it is negative.

Considering that the function of the front and rear differential driving torque is to produce the front and rear wheel steering angle, respectively, and the larger the wheel steering angle, the greater the differential driving torque required. Therefore, it can be approximately considered that there is the following proportional relationship.

$$k = \frac{\delta_f}{\delta_r} = \frac{\Delta M_f}{\Delta M_r} \tag{33}$$

In addition, the front and rear differential driving torques are also needed to meet the following condition,

$$\Delta M_f + \Delta M_r = \Delta M \tag{34}$$

then the front and rear differential driving torques can be described as

$$\Delta M_f = \frac{k}{k+1}\Delta M, \quad \Delta M_r = \frac{1}{k+1}\Delta M \tag{35}$$

## VI. SIMULANTION RESULTS AND ANALYSIS

The characteristics of the 4WSV is that the front and rear wheels turn in the reverse direction at low speed, and turn in the same direction at high speed. In this section, the reference model, 4WSV and 4WDSV with controllers are simulated and compared. The parameters are as follows: $m = 1250$ kg, $I_z = 2031.4$ kg·m$^2$, $k_f = -985950$ N/rad, $k_r = -67312$ N/rad, $l_f = 1.04$ m, $l_r = 1.56$ m, $l_{fm} = 1.0549$ m, $l_{rm} = 1.5451$ m, $l_s = 0.7405$ m, $R = 0.304$ m.

### A. REVERSE PHASE STEERING

The front wheel steering angle of the reference model at the speed of 8.33m/s is a step input with the amplitude of 0.157rad. The reference model and 4WSV with controller are simulated firstly, and their response curves are shown in Figs. 7-9. And Fig. 10 is the obtained MAP of the front and rear wheel steering angles. Then based on the MAP the 4WSV and 4WSDV with controller are simulated, and their response curves are shown in Figs. 11-14.

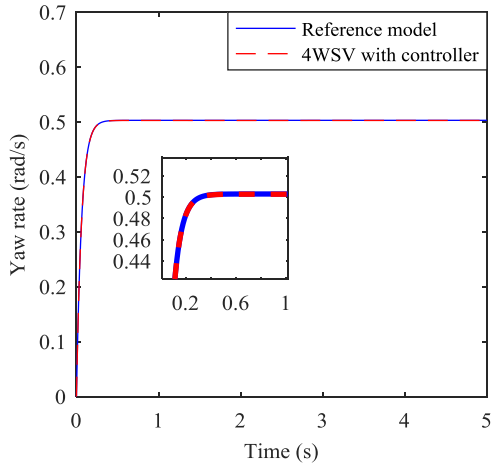


**FIGURE 7.** Yaw rates of different vehicles at 8.33 m/s.

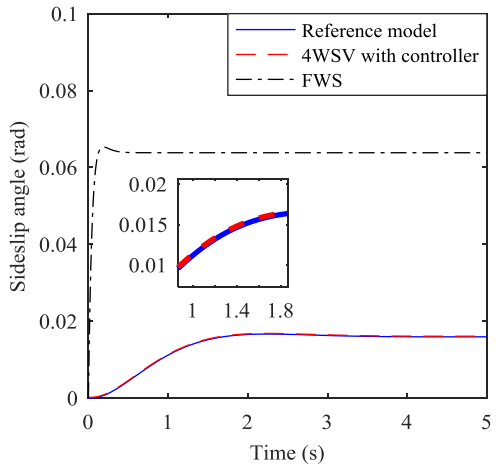


**FIGURE 8.** Sideslip angles of different vehicles at 8.33 m/s.

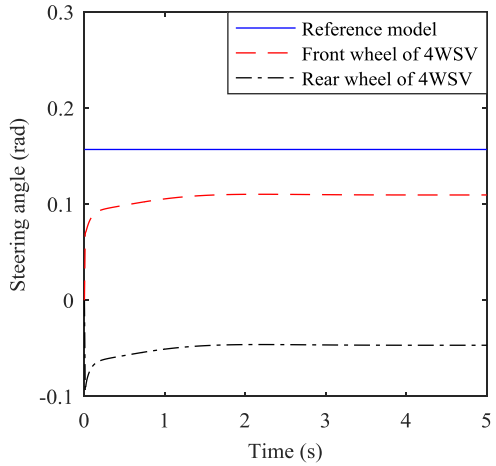


**FIGURE 9.** Steering angles of different vehicles at 8.33 m/s.

From Figs. 7 and 8, it can be seen that the yaw rate and sideslip angle of the 4WSV with the decoupling and fractional $PI^{\lambda}D^{\mu}$ controller can fully track those of the reference model. Also from Fig. 8, we can see that the sideslip angle of the normal FWS is 0.065rad, but that of the reference model is 0.016rad because of the adoption of the drop filter of the sideslip angle.

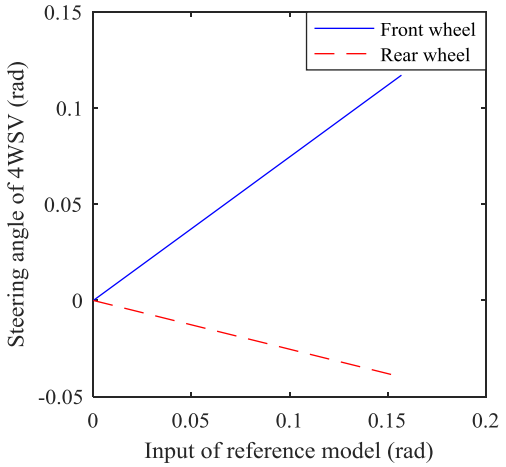


**FIGURE 10.** MAP diagram of 4WSV at 8.33 m/s.

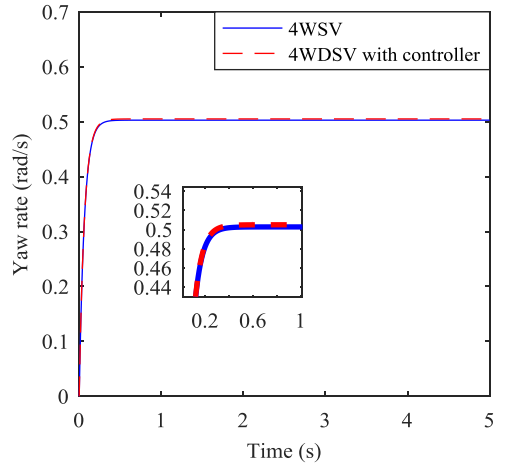


**FIGURE 11.** Yaw rates of different vehicles at 8.33 m/s.

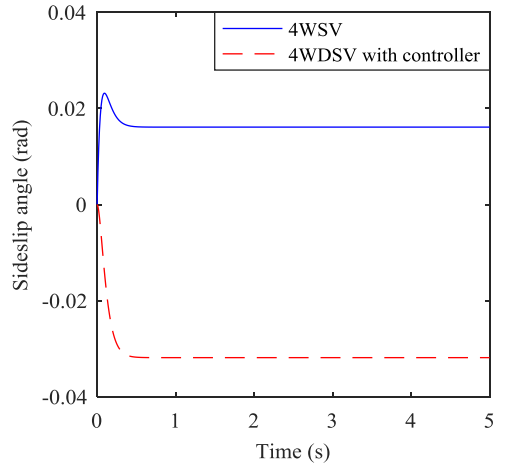


**FIGURE 12.** Sideslip angles of different vehicles at 8.33 m/s.

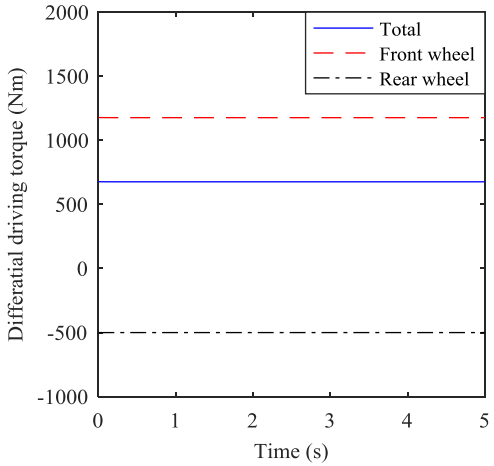


**FIGURE 13.** Differential driving torques of 4WDSV at 8.33 m/s.

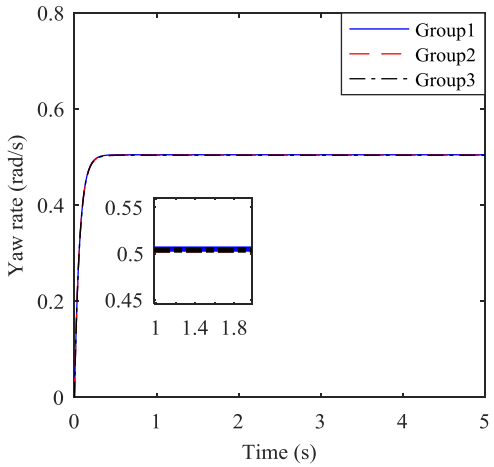


**FIGURE 14.** Yaw rates of 4WDSV with different parameters.

And Fig. 9 shows that the front and rear wheel steering angles of the 4WSV with controllers are 0.1097rad and -0.0467rad respectively, which indicates that the front and rear wheels do rotate in reverse direction to meet the requirement of maneuverability at low speed. And the required front wheel steering angle decreases obviously because of the rear wheel rotates in the opposite direction. Therefore, the standard front and rear wheel steering angles of the 4WSV can be obtained based on the different inputs of the reference model by the decoupling and fractional PID control of 4WSV. When the vehicle speed is fixed and the input of the reference model is changed, a series of front and rear wheel angles of the 4WSV can be obtained. And the MAP diagram at 8.33m/s is shown in Fig. 10. When the driver's steering signal is collected, the ECU can consult the corresponding front and rear wheel angle of the 4WSV on the MAP.

From Figs. 11-13, it can be seen that the yaw rate of the 4WSV can be followed exactly by the 4WDSV with controller although their sideslip angles are different with each other. And the total, front wheel and rear wheel differential driving torques required to realize the 4WDS are 676, 1177 and −501N·m respectively, as shown in Fig. 13.

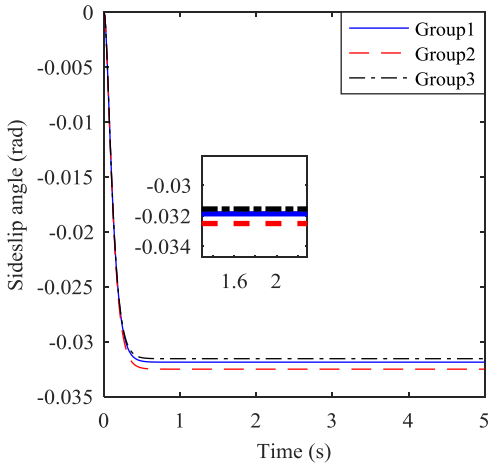


**FIGURE 15.** Sideslip angles of 4WDSV with different parameters.

Figs. 14 and 15 are the yaw rate and sideslip angle curves of the 4WDSV with three groups of different parameters, where Group 1 denotes the nominal parameters, Group 2 and Group 3 represent the parameters in which all of the vehicle mass, yaw moment of inertia, front and rear tire cornering stiffness are decreased and increased by 5% respectively as other parameters remain unchanged. And from Figs. 14-15, it is easy to draw a conclusion that the SMC demonstrates good robustness.

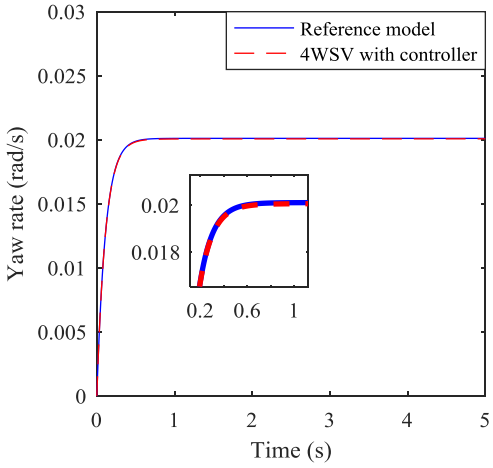


**FIGURE 16.** Yaw rates of different vehicles at 30 m/s.

### *B. IN PHASE STEERING*

At the speed of 30m/s, the front wheel steering angle of the reference model is the step input with the amplitude of 0.00174rad. The reference model and 4WSV with controller are simulated, and Figs. 16-19 show their response curves. The obtained MAP of the front and rear wheel steering angles is shown in Fig. 20. Then the simulation of the 4WSV and 4WSDV with controller are carried out, and their response curves are shown in Figs. 21-23.

It can be drawn from Figs. 16 and 17 that both of the yaw rate and sideslip angle of the reference model can be

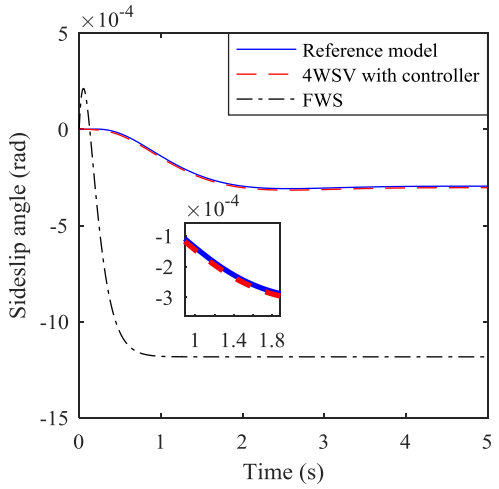


**FIGURE 17.** Sideslip angles of different vehicles at 30 m/s.

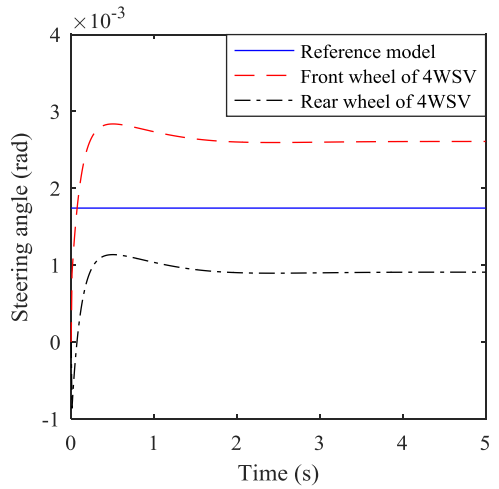


**FIGURE 18.** Steering angles of different vehicles at 30 m/s.

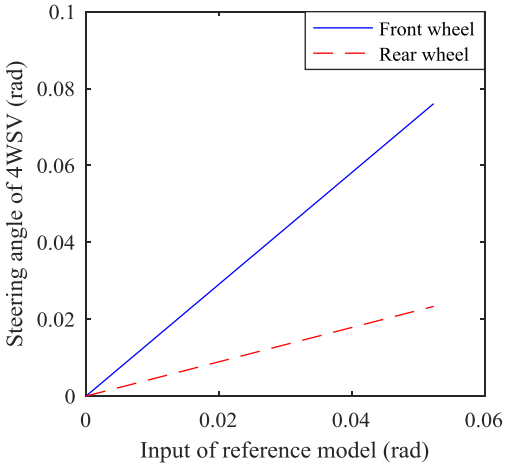


**FIGURE 19.** MAP diagram of 4WSV at 30 m/s.

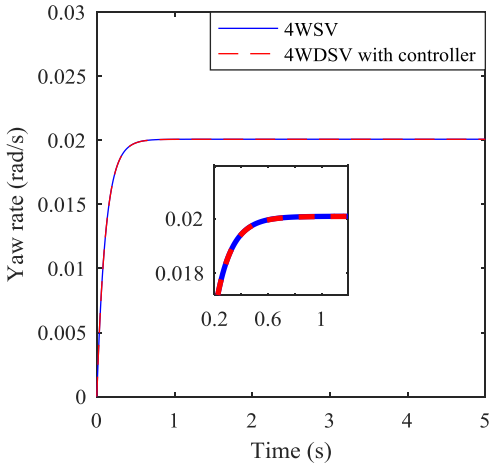


**FIGURE 20.** Yaw rates of different vehicles at 30 m/s.

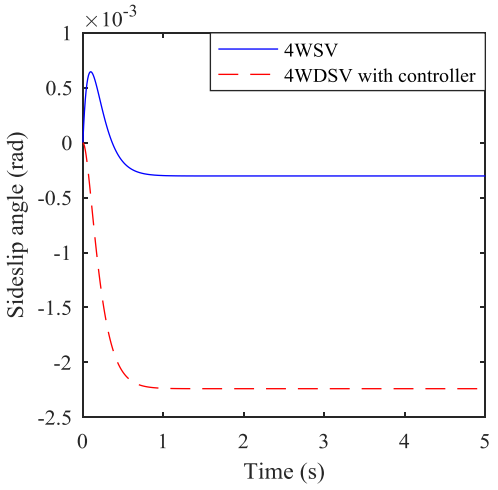


**FIGURE 21.** Sideslip angles of different vehicles at 30 m/s.

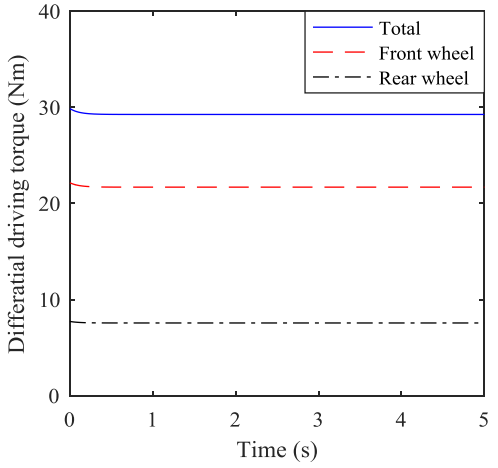


**FIGURE 22.** Differential driving torques of 4WDSV at 30 m/s.

completely followed by the 4WSV with the decoupling and fractional $PI^{\lambda}D^{\mu}$ controller, which indicates that the designed controller of the 4WSV is effective. Also from Fig. 17, we can see that the sideslip angle of the reference model is far less than that of the normal FWS because the drop filter of the sideslip angle is adopted.

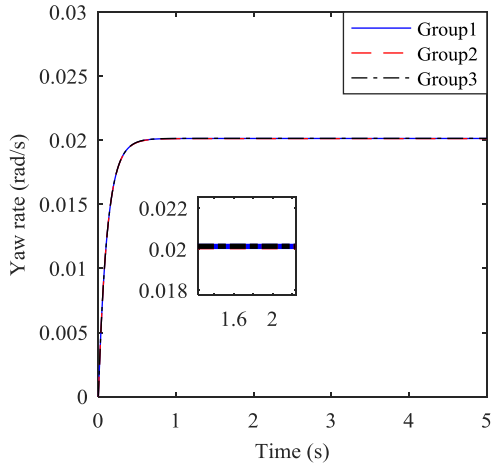


**FIGURE 23.** Yaw rates of 4WDSV with different parameters.

Fig. 18 shows that the standard front and rear wheel steering angles of the 4WSV having the same steering characteristics as the reference model, are 0.00261rad and 0.00091rad respectively, which indicates that at high speed the front and rear wheels do rotate in the same direction to meet the requirement of handling stability. And the required front wheel steering angle increases obviously because of the rear wheel rotates in the same direction. When the vehicle speed is fixed, a series of front and rear wheel angles of the 4WSV can be obtained with the change of the input of the reference model. And the MAP diagram at 30m/s is shown in Fig. 19, which can be consulted by the ECU according to the drive's steering signal.

It can be seen from Figs. 20-21 that the yaw rate of the 4WDSV with SMC controller has almost the same as that of 4WSV, although their sideslip angles are different from each other. And the required total, front wheel and rear wheel differential driving torques are 29.2, 21.7 and 7.5N·m, respectively, as shown in Fig. 22.

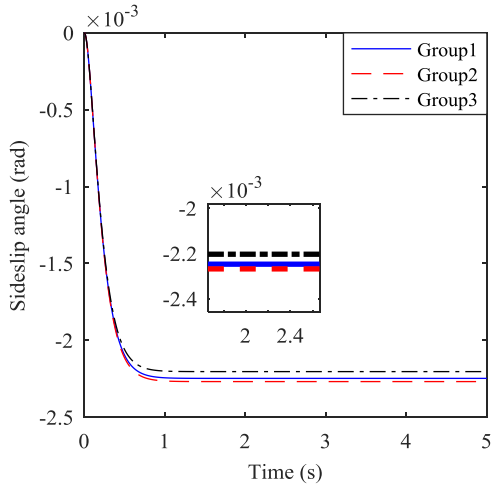


**FIGURE 24.** Sideslip angles of 4WDSV with different parameters.

Figs. 23 and 24 show the yaw rate and sideslip angle of the 4WDSV with three groups of different parameters, which indicates the good robustness of the SMC.

From the above analysis, we can draw a conclusion that the decoupling and fractional $PI^{\lambda}D^{\mu}$ controller for the 4WSV is effective to obtain its standard inputs, and the SMC and torque distributor for the 4WDSV can make its yaw rate completely track that of the 4WSV and also demonstrate good robustness. In conclusion, the proposed control strategy of the 4WDSV is feasible.

## VII. CONCLUSION

The control of the four-wheel differential steering is studied:

(1) Simulation results show that the decoupling and fractional $PI^{\lambda}D^{\mu}$ control can guarantee the 4WSV have the same steering characteristics as the reference model, which indicates that the method to obtain the MAP of the front and rear wheel steering angles at different speed in advance is effective.

(2) Simulation results indicate that the proposed sliding mode controller can ensure the 4WDSV to achieve the same yaw rate as the 4WSV at different speeds according to the 4WSV based on the MAP, which provide a new idea to the solution.

(3) In the future researches, the vehicle roll motion, tire nonlinearity, actuator limitations, and road adhesion coefficient can also be considered.

## REFERENCES

[1] H. Pan and R. S. Song, "The control strategy and experimental analysis of electronic differential steering for four independent drive hub motor electric vehicle," *Adv. Mater. Res.*, vols. 1030–1032, pp. 1550–1553, Dec. 2014.

[2] S. Sakai, H. Sado, and Y. Hori, "Motion control in an electric vehicle with four independently driven in-wheel motors," *IEEE/ASME Trans. Mechatronics*, vol. 4, no. 1, pp. 9–16, Mar. 1999.

[3] W. Li, T. Potter, and R. Jones, "Steering of 4WD vehicles with independent wheel torque control," *Vehicle Syst. Dyn.*, vol. 29, no. 1, pp. 205–218, Jan. 1998.

[4] G. Shuang, N. C. Cheung, K. W. E. Cheng, L. Dong, and X. Liao, "Skid steering in 4-wheel-drive electric vehicle," presented at the 7th Int. Conf. Power Electron. Drive Syst., Bangkok, Thailand, Nov. 30, 2007.

[5] B. Leng, L. Xiong, C. Jin, J. Liu, and Z. Yu, "Differential drive assisted steering control for an in-wheel motor electric vehicle," *SAE Int. J. Passenger Cars-Electron. Electr. Syst.*, vol. 8, no. 2, pp. 433–441, Jan. 2015.

[6] C. Sun, X. Zhang, L. Xi, and Y. Tian, "Design of a path-tracking steering controller for autonomous vehicles," *Energies*, vol. 11, no. 6, p. 1451, Jun. 2018.

[7] J. Wang, Q. Wang, L. Jin, and C. Song, "Independent wheel torque control of 4WD electric vehicle for differential drive assisted steering," *Mechatronics*, vol. 21, no. 1, pp. 63–76, Jun. 2011.

[8] W. Z. Zhao, Y. J. Li, C. Y. Wang, Z. Q. Zhang, and C. L. Xu, "Research on control strategy for differential steering system based on h mixed sensitivity," *Int. J. Automot. Technol.*, vol. 14, no. 6, pp. 913–919, Dec. 2013.

[9] M. Tian, L. Cong, C. Hu, J. Wang, C. Nan, and R. Wang, "Robust $H_{\infty}$ output-feedback yaw control for in-wheel-motor driven electric vehicles with differential steering," *Neurocomputing*, vol. 173, no. 3, pp. 676–684, Jan. 2016.

[10] C. Hu, R. Wang, F. Yan, and H. R. Karimi, "Robust composite nonlinear feedback path-following control for independently actuated autonomous vehicles with differential steering," *IEEE Trans. Transport. Electrific.*, vol. 2, no. 3, pp. 312–321, Sep. 2016.

[11] C. Hu, R. Wang, F. Yan, Y. Huang, H. Wang, and C. Wei, "Differential steering based yaw stabilization using ISMC for independently actuated electric vehicles," *IEEE Trans. Intell. Transp. Syst.*, vol. 19, no. 2, pp. 627–638, Feb. 2018.

[12] J. Tian, J. Tong, and S. Luo, "Differential steering control of four-wheel independent-drive electric vehicles," *Energies*, vol. 11, no. 11, p. 2892, Oct. 2018.

[13] Y. Wang, C. Zong, H. Guo, and H. Chen, "Fault-tolerant path-following control for in-wheel-motor-driven autonomous ground vehicles with differential steering," *Asian J. Control*, vol. 22, no. 3, pp. 1230–1240, Jan. 2019.
[14] H. Jing, R. Wang, C. Li, and J. Wang, "Differential steering-based electric vehicle lateral dynamics control with rollover consideration," *Proc. Inst. Mech. Eng. I, J. Syst. Control Eng.*, vol. 234, no. 3, pp. 338–348, Jul. 2019.
[15] C. Hu, Y. Qin, H. Cao, X. Song, K. Jiang, J. J. Rath, and C. Wei, "Lane keeping of autonomous vehicles based on differential steering with adaptive multivariable super-twisting control," *Mech. Syst. Signal Process.*, vol. 125, pp. 330–346, Jun. 2019.
[16] M. Kuslits and D. Bestle, "Modelling and control of a new differential steering concept," *Vehicle Syst. Dyn.*, vol. 57, no. 4, pp. 520–542, May 2018.
[17] M. A. Khan, M. F. Aftab, E. Ahmed, and I. Youn, "Robust differential steering control system for an independent four wheel drive electric vehicle," *Int. J. Automot. Technol.*, vol. 20, no. 1, pp. 87–97, Feb. 2019.
[18] Y. Shen, B. Zhang, H. Liu, Y. Cui, F. Hussain, S. He, and F. Hu, "Design and development of a novel independent wheel torque control of 4WD electric vehicle," *Mechanics*, vol. 25, no. 3, pp. 210–218, Jul. 2019.
[19] I. Podlubny, "Fractional order systems and $PI^{\lambda}D^{\mu}$ controllers," *IEEE Trans. Autom. Control*, vol. 44, no. 1, pp. 208–214, Feb. 1999.
[20] N. Chen, N. Chen, and Y. Chen, "On fractional control method for four-wheel-steering vehicle," *Sci. China E, Technol. Sci.*, vol. 52, no. 3, pp. 603–609, Mar. 2009.
[21] A. Oustaloup, F. Levron, B. Mathieu, and F. M. Nanot, "Frequency-band complex noninteger differentiator: Characterization and synthesis," *IEEE Trans. Circuits Syst. I, Fundam. Theory Appl.*, vol. 47, no. 1, pp. 25–39, Jan. 2000.

**JIE TIAN** received the B.S. degree in mechanical engineering and automobile engineering, and the M.S. degree in mechanics from the Wuhan University of Technology, Wuhan, China, in 1995 and 1998, respectively, the Ph.D. degree in vehicle engineering from Jiangsu University, in 2011, and the postdoctoral degree in mechanical engineering from Nanjing Forestry university, Nanjing, China, in 2017. From 2015 to 2016, she was a Senior Visiting Scholar with Texas Tech University, USA. She is currently an Associated Professor with Nanjing Forestry University. Her current research interests include vehicle system dynamics and control, and vehicle design CAD/CAE.

**JIE DING** received the B.S. degree in vehicle engineering from Nanjing Forestry University, Nanjing, China, in 2018, where she is currently pursuing the M.S. degree in vehicle engineering with the Department of Traffic and Transportation. Her research interests include the vehicle system dynamics and control.

**CHUNTAO ZHANG** received the B.S. degree from the Zijin College, Nanjing University of Science and Technology, Nanjing, China, in 2018. He is currently pursuing the M.S. degree in vehicle engineering with the Department of Traffic and Transportation, Nanjing Forestry University, Nanjing. His research interests include vehicle system dynamics and control.

**SHI LUO** received the B.S. degree in automatic control and the M.S. and Ph.D. degrees in vehicle engineering from Jiangsu University, Zhengjiang, China, in 1992, 2002, and 2010, respectively. He is currently an Associated Professor with Jiangsu University. His current research interests include vehicle system dynamics and control, and automotive electronics.